Period-doubling bifurcation in two-stage power factor correction converters using the method of incremental harmonic balance and Floquet theory*

Wang Fa-Qiang(王发强)†, Zhang Hao(张 浩), and Ma Xi-Kui(马西奎)

State Key Laboratory of Electrical Insulation and Power Equipment, School of Electrical Engineering, Xi'an Jiaotong University, Xi'an 710049, *China*

(Received 18 July 2011; revised manuscript received 15 September 2011)

In this paper, period-doubling bifurcation in a two-stage power factor correction converter is analyzed by using the method of incremental harmonic balance (IHB) and Floquet theory. A two-stage power factor correction converter typically employs a cascade configuration of a pre-regulator boost power factor correction converter with average current mode control to achieve a near unity power factor and a tightly regulated post-regulator DC–DC Buck converter with voltage feedback control to regulate the output voltage. Based on the assumption that the tightly regulated post-regulator DC–DC Buck converter is represented as a constant power sink and some other assumptions, the simplified model of the two-stage power factor correction converter is derived and its approximate periodic solution is calculated by the method of IHB. And then, the stability of the system is investigated by using Floquet theory and the stable boundaries are presented on the selected parameter spaces. Finally, some experimental results are given to confirm the effectiveness of the theoretical analysis.

Keywords: two-stage power factor correction converter, incremental harmonic balance, Floquet theory, period-doubling bifurcation

PACS: 05.45.–a, 84.30.Jc, 45.10.Hj **DOI:** 10.1088/1674-1056/21/2/020505

1. Introduction

In engineering applications, the power factor correction (PFC) converter is one of the basic requirements of power systems since it can force the input current to follow the input voltage to obtain a near unity power factor. Therefore, many topologies of PFC converter and various control methods have been proposed in Refs. [1]–[7]. In general, by considering tight output regulation, there are two types of typical active PFC converter,[5−7] i.e., single-stage PFC converter, and two-stage PFC converter. For the single-stage PFC converter, the pre-regulator PFC converter and the post-regulator DC–DC converter share the same control circuit to reduce the cost and complexity. However, the low efficiency and the variation of the bulk capacitor voltage lead to its limitation in practice. For the two-stage PFC converter, the pre-regulator PFC converter and the post-regulator DC–DC converter has its own control circuit, and accordingly it can achieve both power factor correction and output regulation, and this leads to many advantages, such as low total harmonic distortion (THD), high power factor, and constant bulk capacitor voltage. Thus, the modeling, dynamical behaviours, and control methods of the two-stage PFC converter have received a great deal of attention. Especially, since the complex behaviours in PFC converter will have an adverse effect on its performance,[8−17] the complex behaviours in the two-stage PFC converter have also been more and more concerned in recent years.[18−21] For example, Orabi *et al.* pointed out that the period-doubling bifurcation, which occurs at the line frequency, could be observed in the two-stage PFC converter through computer aided simulations and circuit experiments.[18] Chu *et al.* proposed the double-averaging method to analyse this period-doubling bifurcation theoretically and gave the critical condition of the stable operation for practical design.[20] However, if the accuracy of the results is highly improved

*Project supported by the National Natural Science Foundation of China (Grant No. 51007068), the Specialized Research Fund for the Doctoral Program of Higher Education of China (Grant No. 20100201120028), the Fundamental Research Funds for the Central Universities of China, and the State Key Laboratory of Electrical Insulation and Power Equipment of China (Grant No. EIPE10303).

†Corresponding author. E-mail: faqwang@mail.xjtu.edu.cn

© 2012 Chinese Physical Society and IOP Publishing Ltd

or the original system is very complex, the double-averaging method may be too difficult to identify the type of instability. Most importantly, the two-stage PFC converter is a periodic structural vibration and thus the solution of the system is also periodic. Accordingly, if we use a more general method to directly analyse the stability of the periodic orbit of the system, the results will be more straightforward and easier to understand. Note that only the period-doubling bifurcation at the line frequency, which is generally called slow-scale instability,[18−20] is concerned with in this paper.

The incremental harmonic balance (IHB), which was originally developed by Lau *et al.*[22] for treating periodic structural vibrations and widely applied to tackle different kinds of dynamic problems,[23−27] is a semi-analytical method and is remarkably effective in computer implementation for obtaining the periodic solutions. For example, Ge *et al.* utilised the method of IHB and Floquet theory to investigate the bifurcation and chaotic responses in a single-axis rate gyro mounted on a space vehicle.[23] Raghothama *et al.* used the IHB to investigate the periodic motions of nonlinearly geared rotor-bearing system.[24] The method was also applied by Shen *et al.* to investigate the bifurcation and the route-to-chaos of Mathieu–Duffing oscillator.[27] In this paper, we apply the method of IHB and Floquet theory to investigate the period-doubling bifurcation in the two-stage PFC converter, i.e., the approximate periodic solution of the simplified model is calculated by the IHB, and the stability of the system is identified by using the Floquet theory.

The rest of the paper is organized as follows. In the next section, the simplified model of the two-stage PFC converter under some assumptions is derived. In Section 3, the approximate periodic solution of the simplified model is calculated by the IHB and the stability of the system is identified by Floquet theory. In Section 4, the period-doubling bifurcation in the circuit system is analysed and some typical figures are given. In Section 5, some experimental data are given to confirm the effectiveness of the method of IHB and Floquet theory. Finally, some concluding remarks and comments are given in Section 6.

2. Two-stage PFC converter and its simplified model

A two-stage PFC converter typically consists of a pre-regulator Boost PFC converter with average current mode (ACM) control and a post-regulator DC–DC Buck converter with voltage feedback control, as depicted in Fig. 1. Obviously, this system is a rather complex nonlinear one for theoretical analysis. Fortunately, if the DC–DC Buck converter is well controlled, the tightly regulated DC–DC Buck converter under a fixed load condition can be replaced by a constant power sink,[18,20] and its detail is shown in Fig. 2. Note that the ACM control is usually realized by IC UC3854.[28]

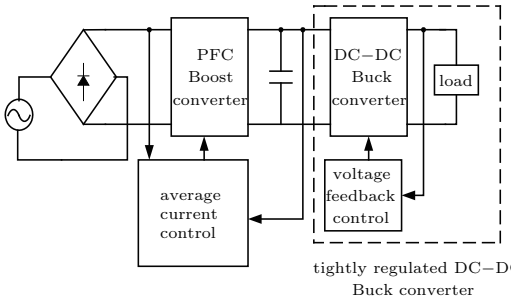


Fig. 1. Schematic of the two-stage PFC converter.

The constant power sink can be described as follows.

$$i_{\rm PFC} = \frac{P_0}{\eta v_{\rm PFC}}, \tag{1}$$

where $v_{\rm PFC}$ is the output voltage of the pre-regulator boost PFC stage, P_0 is the constant power, $i_{\rm PFC}$ is the current through the constant power sink, and η is the efficiency of the DC–DC Buck converter. One can see that the constant power sink has a negative impedance characteristic since the current $i_{\rm PFC}$ decreases when the voltage $v_{\rm PFC}$ increases, and *vice versa*. This is different from a pre-regulator PFC converter with a resistive load, so that we cannot simply extend the stability conditions of a pre-regulator PFC converter with a resistive load to a practical two-stage PFC converter.[19] In other words, the stability of the two-stage PFC converter should be reconsidered completely.

The system in Fig. 2. is also a high order piecewise one with low frequency excitation signal even if the post-regulator DC–DC Buck converter is replaced by a constant power sink. Thus, without losing the main dynamical behaviours, the following two assumptions should be made for simplicity.

(i) All the components in the system are regarded as ideal and the voltage across the sensing resistor $R_{\rm s}$ is ignored. Also, the efficiency of the DC–DC Buck converter is assumed to be 100%, i.e., $\eta \approx 1$. Additionally, the output of the second-order filter $v_{\rm ff}$ is regarded as a constant value since its ripple is very

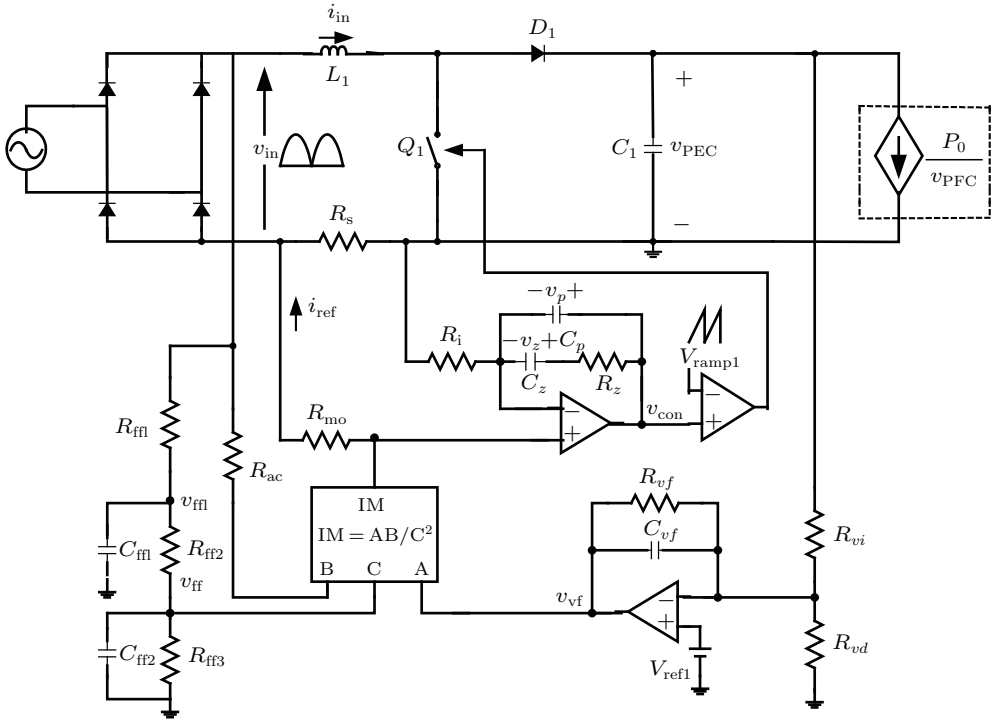


Fig. 2. Boost PFC converter terminated by a constant power sink.

small. Its value is[28]

$$V_{\rm ff} = \frac{0.9R_{\rm ff3}}{R_{\rm ff1}+R_{\rm ff2}+R_{\rm ff3}}V_{\rm in}, \tag{2}$$

where $V_{\rm in}$ is the root-mean-square (rms) value of the input voltage.

(ii) The system only operates in continuous conduction mode (CCM). Also, if only the period-doubling bifurcation occurring at the line frequency is considered and the current compensator is well designed, the current $i_{\rm in}$ can be considered as following the current programming signal $i_{\rm ref}$ linearly.[20]

Under the above two assumptions, the simplified model can be obtained as

$$\begin{cases} \dfrac{{\rm d}v_{vf}}{{\rm d}t} = -\dfrac{v_{vf}}{C_{vf}R_{vf}} + \Big(\dfrac{1}{C_{vf}R_{vf}} + \dfrac{R_{vi}+R_{vd}}{R_{vi}R_{vd}C_{vf}}\Big)V_{\rm ref1} \\ \qquad\qquad -\dfrac{1}{R_{vi}C_{vf}}v_{\rm PFC}, \\ \dfrac{{\rm d}v_{\rm PFC}}{{\rm d}t} = -\dfrac{P_0}{C_1 v_{\rm PFC}} \\ \qquad\qquad +\dfrac{R_{\rm mo}V_{\rm in}^2(1-\cos(2\omega_l t))}{R_s V_{\rm ff}^2 R_{ac} C_1 v_{\rm PFC}}(v_{vf}-1), \end{cases} \tag{3}$$

where ω_l is the angular frequency, v_{vf} is the output voltage of the voltage compensator of the ACM control, and $V_{\rm ref1}$ is the desired reference voltage of the pre-regulator boost PFC stage. Obviously, the obtained simplified model is a nonlinear non-autonomous system.

3. Theoretical derivations

First, the periodic solution of the simplified model of the two-stage PFC converter is derived by using the IHB method. And then, the stability of the circuit system is identified by using Floquet theory.

3.1. Formulation for IHB

Let $\omega_0 = 2\omega_l$ and $\tau = \omega_0 t$. the simplified model (3) of the two-stage PFC converter can be rewritten as follows:

$$\begin{cases} v'_{vf} = -\dfrac{\alpha}{\omega_0}v_{vf} + \dfrac{F_1}{\omega_0} - \dfrac{\beta}{\omega_0}v_{\rm PFC}, \\ v'_{\rm PFC} = -\dfrac{F_2}{\omega_0 v_{\rm PFC}} + \dfrac{\gamma}{\omega_0 v_{\rm PFC}}(v_{vf}-1)(1-\cos(\tau)), \end{cases} \tag{4}$$

where $v'_{vf} = {\rm d}v_{vf}/{\rm d}\tau$, $v'_{\rm PFC} = {\rm d}v_{\rm PFC}/{\rm d}\tau$, $\alpha = 1/C_{vf}R_{vf}$, $\beta = 1/R_{vi}C_{vf}$, $\gamma = R_{\rm mo}V_{\rm in}^2/C_1R_{\rm s}V_{\rm ff}^2R_{\rm ac}$,

$$F_1 = \Big(\frac{1}{C_{vf}R_{vf}} + \frac{R_{vi}+R_{vd}}{R_{vi}R_{vd}C_{vf}}\Big)V_{\rm ref1},$$

and $F_2 = P_0/C_1$.

From the first equation of Eq. (4), the solution for $v_{\rm PFC}$ can be derived as

$$v_{\rm PFC} = -\frac{\omega_0}{\beta}v'_{vf} - \frac{\alpha}{\beta}v_{vf} + \frac{F_1}{\beta}. \tag{5}$$

Substituting Eq. (5) into the second equation of Eq. (4) yields

$$\omega_0^3 v''_{vf} v'_{vf} + \alpha\omega_0^2 (v'_{vf})^2 + \alpha\omega_0^2 v''_{vf} v_{vf} + \alpha^2\omega_0 v'_{vf} v_{vf} - F_1\omega_0^2 v''_{vf} - F_1\alpha\omega_0 v'_{vf} = -\beta^2 F_2 + \beta^2\gamma(v_{vf}-1)(1-\cos(\tau)), \quad (6)$$

where $v''_{vf} = \mathrm{d}^2 v_{vf}/\mathrm{d}\tau^2$.

Let

$$v_{vf} = V_{vf} + \Delta v_{vf}, \quad (7)$$

where V_{vf} is the guessed solution and Δv_{vf} is the incremental part. By substituting Eq. (7) into Eq. (6) and ignoring the higher-order terms of Δv_{vf} since their values are very small, the following incremental equation is derived

$$K_1\Delta v''_{vf} + K_2\Delta v'_{vf} + K_3\Delta v_{vf} = M_1 + M_2, \quad (8)$$

where

$$K_1 = (\omega_0^3 V'_{vf} + \alpha\omega_0^2 V_{vf} - F_1\omega_0^2), \quad (9)$$

$$K_2 = \omega_0^3 V''_{vf} + \alpha\omega_0^2 V'_{vf} + \alpha\omega_0^2 V'_{vf} + \alpha^2\omega_0 V_{vf} - F_1\alpha\omega_0, \quad (10)$$

$$K_3 = \alpha\omega_0^2 V''_{vf} + \alpha^2\omega_0 V'_{vf} - \gamma\beta^2(1-\cos(\tau)), \quad (11)$$

$$M_1 = -\omega_0^3 V''_{vf} V'_{vf} - \alpha\omega_0^2 V''_{vf} V_{vf} + F_1\omega_0^2 V''_{vf} - \alpha\omega_0^2 V'_{vf} V'_{vf} - \alpha^2\omega_0 V'_{vf} V_{vf} + F_1\alpha\omega_0 V'_{vf}, \quad (12)$$

$$M_2 = -\beta^2 F_2 + \beta^2\gamma(1-\cos(\tau))(V_{vf}-1). \quad (13)$$

Let the voltage V_{vf} and Δv_{vf} be expressed in the following harmonic series of τ

$$V_{vf} = a_0 + \sum_{n=1}^{N} [a_n\cos(n\tau) + b_n\sin(n\tau)], \quad (14)$$

$$\Delta v_{vf} = \Delta a_0 + \sum_{n=1}^{N} [\Delta a_n\cos(n\tau) + \Delta b_n\sin(n\tau)], \quad (15)$$

where N is a natural number and is to be determined in the required accuracy, Δa_n and Δb_n are the increments of a_n and b_n, respectively.

Define

$$\boldsymbol{E} = \big[\cos(0), \cos(\tau), \ldots, \cos(N\tau), \sin(\tau), \ldots, \sin(N\tau)\big], \quad (16)$$

$$\boldsymbol{A} = [a_0, a_1, \ldots, a_N, b_1, \ldots, b_N], \quad (17)$$

$$\Delta\boldsymbol{A} = [\Delta a_0, \Delta a_1, \ldots, \Delta a_N, \Delta b_1, \ldots, \Delta b_N]. \quad (18)$$

Thus

$$\boldsymbol{E}' = [0, -\sin(\tau), \ldots, -N\sin(N\tau), \cos(\tau), \ldots, N\cos(N\tau)], \quad (19)$$

$$\boldsymbol{E}'' = [0, -\cos(\tau), \ldots, -N^2\cos(N\tau), -\sin(\tau), \ldots, -N^2\sin(N\tau)]. \quad (20)$$

Hence

$$V_{vf} = \boldsymbol{E}\boldsymbol{A}^{\mathrm{T}}, \quad V'_{vf} = \boldsymbol{E}'\boldsymbol{A}^{\mathrm{T}}, \quad V''_{vf} = \boldsymbol{E}''\boldsymbol{A}^{\mathrm{T}}, \quad (21)$$

$$\Delta v_{vf} = \boldsymbol{E}\Delta\boldsymbol{A}^{\mathrm{T}}, \quad \Delta v'_{vf} = \boldsymbol{E}'\Delta\boldsymbol{A}^{\mathrm{T}}, \quad \Delta v''_{vf} = \boldsymbol{E}''\Delta\boldsymbol{A}^{\mathrm{T}}. \quad (22)$$

Substituting Eqs. (21) and (22) into Eqs. (8)–(13) respectively, the following equations can be obtained

$$K_1\boldsymbol{E}''\Delta\boldsymbol{A}^{\mathrm{T}} + K_2\boldsymbol{E}'\Delta\boldsymbol{A}^{\mathrm{T}} + K_3\boldsymbol{E}\Delta\boldsymbol{A}^{\mathrm{T}} = M_1 + M_2, \quad (23)$$

$$K_1 = (\omega_0^3\boldsymbol{E}'\boldsymbol{A}^{\mathrm{T}} + \alpha\omega_0^2\boldsymbol{E}\boldsymbol{A}^{\mathrm{T}} - F_1\omega_0^2), \quad (24)$$

$$K_2 = \omega_0^3\boldsymbol{E}''\boldsymbol{A}^{\mathrm{T}} + 2\alpha\omega_0^2\boldsymbol{E}'\boldsymbol{A}^{\mathrm{T}} + \alpha^2\omega_0\boldsymbol{E}\boldsymbol{A}^{\mathrm{T}} - F_1\alpha\omega_0, \quad (25)$$

$$K_3 = \alpha\omega_0^2\boldsymbol{E}''\boldsymbol{A}^{\mathrm{T}} + \alpha^2\omega_0\boldsymbol{E}'\boldsymbol{A}^{\mathrm{T}} - \gamma\beta^2(1-\cos(\tau)), \quad (26)$$

$$M_1 = -\omega_0^3\boldsymbol{E}''\boldsymbol{A}^{\mathrm{T}}\boldsymbol{E}'\boldsymbol{A}^{\mathrm{T}} - \alpha\omega_0^2\boldsymbol{E}''\boldsymbol{A}^{\mathrm{T}}\boldsymbol{E}\boldsymbol{A}^{\mathrm{T}} + F_1\omega_0^2\boldsymbol{E}''\boldsymbol{A}^{\mathrm{T}} - \alpha\omega_0^2\boldsymbol{E}'\boldsymbol{A}^{\mathrm{T}}\boldsymbol{E}'\boldsymbol{A}^{\mathrm{T}} - \alpha^2\omega_0\boldsymbol{E}'\boldsymbol{A}^{\mathrm{T}}\boldsymbol{E}\boldsymbol{A}^{\mathrm{T}} + F_1\alpha\omega_0\boldsymbol{E}'\boldsymbol{A}^{\mathrm{T}}, \quad (27)$$

$$M_2 = -\beta^2 F_2 + \beta^2\gamma(1-\cos(\tau))(\boldsymbol{E}\boldsymbol{A}^{\mathrm{T}} - 1). \quad (28)$$

With the implementation of the Galerkin procedure,[27] the differential equation of the system becomes

$$\int_0^{2\pi} \boldsymbol{E}^{\mathrm{T}}(K_1\boldsymbol{E}'' + K_2\boldsymbol{E}' + K_3\boldsymbol{E})\Delta\boldsymbol{A}^{\mathrm{T}}\,\mathrm{d}\tau = \int_0^{2\pi} \boldsymbol{E}^{\mathrm{T}}(M_1 + M_2)\,\mathrm{d}\tau. \quad (29)$$

Since the term $\Delta\boldsymbol{A}^{\mathrm{T}}$ has no relation to τ, the above expression can be changed into the following form

$$\boldsymbol{K}\Delta\boldsymbol{A}^{\mathrm{T}} = \boldsymbol{M}, \quad (30)$$

where

$$\boldsymbol{K} = \int_0^{2\pi} \boldsymbol{E}^{\mathrm{T}}(K_1\boldsymbol{E}'' + K_2\boldsymbol{E}' + K_3\boldsymbol{E})\,\mathrm{d}\tau, \quad (31)$$

$$\boldsymbol{M} = \int_0^{2\pi} \boldsymbol{E}^{\mathrm{T}}(M_1 + M_2)\,\mathrm{d}\tau. \quad (32)$$

Also, since the matrix $\boldsymbol{K}$ is full rank, the values for $\Delta\boldsymbol{A}^{\mathrm{T}}$ can be derived by multiplying both sides of the Eq. (30) by $\boldsymbol{K}^{-1}$, i.e.,

$$\Delta\boldsymbol{A}^{\mathrm{T}} = \boldsymbol{K}^{-1}\boldsymbol{M}. \quad (33)$$

First of all, an initial guess of the coefficients in $\boldsymbol{A}^{\mathrm{T}}$ is centred upon Eq. (33) and the solution to $\Delta\boldsymbol{A}^{\mathrm{T}}$ is found. The solution to $\Delta\boldsymbol{A}^{\mathrm{T}}$ are added to $\boldsymbol{A}^{\mathrm{T}}$ such that

$$\boldsymbol{A}^{\mathrm{T}}_{h+1} = \boldsymbol{A}^{\mathrm{T}}_{h} + \Delta\boldsymbol{A}^{\mathrm{T}}_{h}. \quad (34)$$

The process is ended when the value of $\boldsymbol{M}$ is sufficiently small. In this way, the solution to $\boldsymbol{A}^{\mathrm{T}}$ can be calculated.

3.2. Stability of the periodic solution

After obtaining the solution of $\boldsymbol{A}^{\mathrm{T}}$, the steady state of the simplified model is also obtained, which is in periodic form, and its stability can be investigated by introducing a small perturbation Δv_{PFC} to V_{PFC} and Δv_{vf} to V_{vf}, i.e.,

$$v_{\mathrm{PFC}} = V_{\mathrm{PFC}} + \Delta v_{\mathrm{PFC}}, \tag{35}$$

$$v_{vf} = V_{vf} + \Delta v_{vf}, \tag{36}$$

where V_{vf} has been given in Eq. (14) and V_{PFC} is given as follows:

$$\begin{aligned} V_{\mathrm{PFC}} = \sum_{n=1}^{N} \Big[& \Big(\frac{n a_n \omega_0}{\beta} - \frac{\alpha b_n}{\beta} \Big) \sin(n\tau) \\ & - \Big(\frac{\omega_0 n b_n}{\beta} + \frac{\alpha a_n}{\beta} \Big) \cos(n\tau) \Big] \\ & + \frac{1}{\beta} F_1 - \frac{\alpha}{\beta} a_0. \end{aligned} \tag{37}$$

Thus, the following equations can be obtained by linearization of Eq. (4) at (V_{vf}, V_{PFC}).

$$\boldsymbol{V}' = \boldsymbol{Y}(\tau)\boldsymbol{V}, \quad \boldsymbol{V} = (\Delta v_{vf}, \Delta v_{\mathrm{PFC}})^{\mathrm{T}} \in R^2, \tag{38}$$

where

$$\boldsymbol{Y}(\tau) = \begin{bmatrix} -\dfrac{\alpha}{\omega_0} & -\dfrac{\beta}{\omega_0} \\ \dfrac{\gamma(1-\cos(\tau))}{\omega_0 v_{\mathrm{PFC}}} & \dfrac{F_2 - \gamma(v_{vf}-1)(1-\cos(\tau))}{\omega_0 v_{\mathrm{PFC}}^2} \end{bmatrix}. \tag{39}$$

Obviously, $\boldsymbol{Y}(\tau)$ is a periodic matrix with the same period as (V_{vf}, V_{PFC}), i.e., $\boldsymbol{Y}(\tau+T) = \boldsymbol{Y}(\tau)$. If $\boldsymbol{\Phi}(\tau) = [\boldsymbol{\Phi}_1(\tau), \boldsymbol{\Phi}_2(\tau)]$ is the fundamental solution to Eq. (38), which satisfies the initial condition $\boldsymbol{\Phi}(0) = \boldsymbol{I}$, $\boldsymbol{\Phi}(\tau+T)$ is also the fundamental solution. Therefore, the relation between $\boldsymbol{\Phi}(\tau+T)$ and $\boldsymbol{\Phi}(\tau)$ can be expressed as[27]

$$\boldsymbol{\Phi}(\tau+T) = \boldsymbol{T}_M \boldsymbol{\Phi}(\tau), \tag{40}$$

where $\boldsymbol{T}_M$ is the transition matrix.

By taking $\tau = 0$ and using $\boldsymbol{\Phi}(0) = \boldsymbol{I}$, the transition matrix $\boldsymbol{T}_M$ is written as

$$\boldsymbol{T}_M = \boldsymbol{\Phi}(T). \tag{41}$$

From the calculated eigenvalues of the transition matrix $\boldsymbol{T}_M$, the stability of the system and the type of bifurcation can be determined. If all the eigenvalues are within the unit circle with its centre at the origin of the complex plane, the periodic solution is stable. Otherwise, the periodic solution is unstable. That is, a bifurcation occurs.[29] For example, the period-doubling bifurcation will occur if there is a real eigenvalue moving out of the unit circle in the negative direction (cross at -1) with remaining eigenvalues staying inside the unit circle. The Hopf bifurcation will occur if there is a pair of conjugate eigenvalues moving out of the unit circle with remaining eigenvalues staying inside it.

First, the period T ($= 2\pi$) is divided into N_k subintervals, and the k-th interval is $\Delta_k = t_k - t_{k-1}$, where $t_k = Tk/N_k$. And then, the value of the time-varying $\boldsymbol{Y}(\tau)$ can be approximated to the following constant matrix in the k-th interval when N_k is chosen to be sufficiently large since $\boldsymbol{Y}(\tau)$ is continuous with respect to τ. So, let

$$\boldsymbol{Y}_k = \frac{1}{\Delta_k} \int_{t_{k-1}}^{t_k} \boldsymbol{Y}(\tau)\,\mathrm{d}\tau; \tag{42}$$

the transition matrix $\boldsymbol{T}_M$ is

$$\begin{aligned} \boldsymbol{T}_M &= \prod_{i=N_k}^{1} [\exp(\boldsymbol{Y}_i \boldsymbol{\Delta}_i)] \\ &= \prod_{i=N_k}^{1} \left[\boldsymbol{I} + \sum_{j=1}^{N_j} \frac{(\boldsymbol{Y}_i \Delta_i)^j}{j!} \right], \end{aligned} \tag{43}$$

where N_j denotes the number of terms in the approximation of the constant matrix $\boldsymbol{Y}_k$ exponential and

$$\boldsymbol{Y}_k = \begin{bmatrix} -\dfrac{\alpha}{\omega_0} & -\dfrac{\beta}{\omega_0} \\ \dfrac{1}{\Delta_k} \displaystyle\int_{t_{k-1}}^{t_k} \left[\frac{\gamma(1-\cos(\tau))}{\omega_0 v_{\mathrm{PFC}}} \right] \mathrm{d}\tau & \dfrac{1}{\Delta_k} \displaystyle\int_{t_{k-1}}^{t_k} \frac{F_2 - \gamma(v_{vf}-1)(1-\cos(\tau))}{\omega_0 v_{\mathrm{PFC}}^2}\,\mathrm{d}\tau \end{bmatrix}. \tag{44}$$

From the above derivations, one can see that the stability of the nonlinear non-autonomous system is directly identified by detecting the stability of the obtained approximate periodic solution.

4. Bifurcation analysis

It is necessary to analyse the period-doubling bifurcation in detail so as to understand the nonlinear phenomenon and to determine the boundaries about the stable operation. Note that, since the objective of the pre-regulator PFC converter is to achieve a near-

unity power factor, the higher-order harmonic contents can be ignored, and here we take $N = 3$. Additionally, we take $V_{\rm in} = 75$ V, $f_l = 60$ Hz, $T_{\rm s} = 10.9$ μs, $L_1 = 3$ mH, $R_{\rm s} = 0.5$ Ω, $R_{\rm mo} = 3.9$ kΩ, $R_i = 3.9$ kΩ, $R_{\rm ac} = 620$ kΩ, $R_{vi} = 510$ kΩ, $C_{vf} = 44$ nF, $R_z = 30$ kΩ, $C_p = 220$ pF, $C_z = 1$ nF, $R_{\rm ff1} = 910$ kΩ, $R_{\rm ff2} = 91$ kΩ, $R_{\rm ff3} = 22$ kΩ, $C_1 = 107$ μF, $R_{vd} = 33$ kΩ, and $P_0 = 20$ W.

First, the period-doubling bifurcation is generally investigated as the variation of the resistance R_{vf}. Let $R_{vf} = 150$ kΩ, the approximate periodic solution of the simplified model is calculated by using the IHB, the results are shown as follows:

$$\begin{aligned} V_{vf} =& 1.54248750270047 - 0.106091992117667\cos(\tau) \\ &+ 0.225259934801700 \times 10^{-2}\cos(2\tau) \\ &- 0.165169946946469 \times 10^{-4}\cos(3\tau) \\ &+ 0.257910642836605 \times 10^{-1}\sin(\tau) \\ &- 0.100366762695911 \times 10^{-2}\sin(2\tau) \\ &+ 0.212029740660364 \times 10^{-4}\sin(3\tau), \end{aligned} \tag{45}$$

$$\begin{aligned} V_{\rm PFC} =& 143.664633399909 \\ &- 0.756555641813270 \times 10^{-1}\cos(\tau) \\ &+ 0.263039928190563 \times 10^{-1}\cos(2\tau) \\ &- 0.102006456066546 \times 10^{-2}\cos(3\tau) \\ &- 1.88269837433712\sin(\tau) \\ &+ 0.796375548269231 \times 10^{-1}\sin(2\tau) \\ &- 0.910461119027192 \times 10^{-3}\sin(3\tau). \end{aligned} \tag{46}$$

Meanwhile, by comparing the results from the IHB on the simplified model with the results from the time-integration on the complete model, as plotted in Fig. 3, it is found that it is reasonable and effective to use the simplified model to replace the system terminated by a constant power sink, when the current compensator is well designed, and the IHB is used effectively to calculate the approximate periodic solution of the simplified model. Also, it is reasonable to choose $N = 3$ to describe the approximate periodic solution and to assume that the system only operates in CCM operation.

The eigenvalues of the transition matrix $\boldsymbol{T}_M$ can be obtained: $\lambda_1 = -0.4842046332$, $\lambda_2 = -0.5842778744$. Obviously, the two eigenvalues are staying inside the unit circle, and this leads to stable operation of the system. But, when the value of the resistance R_{vf} is varied, the eigenvalues of the transition matrix $\boldsymbol{T}_M$ may change, as shown in Table 1 and Fig. 4(a).

From Table 1 and Fig. 4(a), it is clear that there is a real eigenvalue moving out of the unit circle in the negative direction (cross by -1) with the remaining eigenvalue staying inside the unit circle for increasing

Table 1. The eigenvalues for different R_{vf}.

R_{vf}/kΩ	λ_1	λ_2	State
150.0	−0.4842046332	−0.5842778744	stable
170.0	−0.4484592726	−0.7318757010	stable
190.0	−0.4448330802	−0.8296477718	stable
210.0	−0.4471104033	−0.9076230096	stable
230.0	−0.4512533897	−0.9726551753	stable
239.4	−0.4534370222	−0.9997797017	stable
239.5	−0.4534606264	−1.0000579450	period-doubling bifurcation
260.0	−0.4583524545	−1.0530372540	unstable

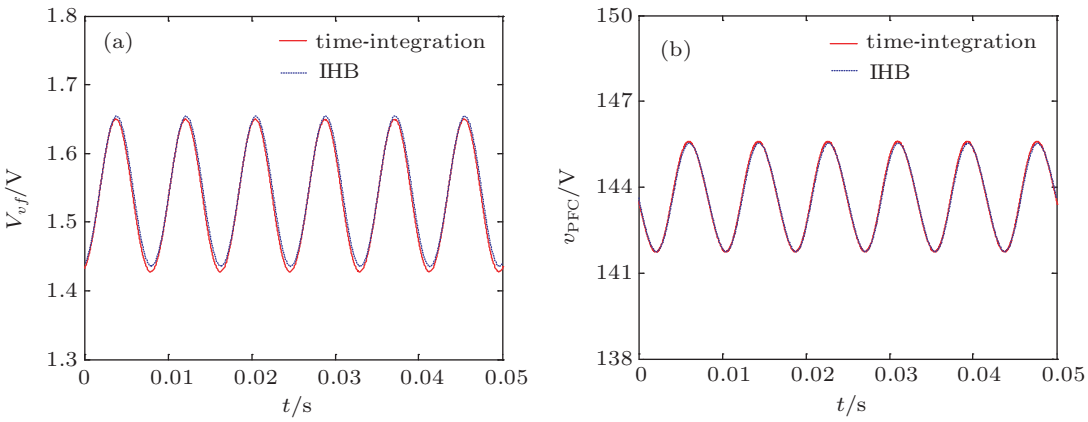


Fig. 3. The solutions of the system by using time-integration for the complete model (solid line) and the IHB for the simplified model (dashed line): (a) the voltage v_{vf} and (b) the voltage $v_{\rm PFC}$.

resistance R_{vf}. This denotes that the period-doubling bifurcation occurs and the bifurcation point is $R_{vf} = 239.5$ kΩ. Therefore, the system will operate in stable operation at $R_{vf} < 239.5$ kΩ. Otherwise, it will be in unstable operation. Also, the above conclusion can be obtained by the bifurcation diagram, as shown in Fig. 4(b).

Furthermore, we record the critical value, at which period-doubling bifurcation occurs, when the other parameters varies at $R_{vf} = 200$ kΩ/250 kΩ, as shown in Figs. 5(a), 5(b), and 5(c). One can observe that the stable region increases as R_{vf} decreases, while the period-doubling bifurcation develops as C_1 decreases (as R_{vd} increases, R_{vi} decreases, the $R_{\rm ff3}$ decreases, the output power P_0 increases, and the C_{vf} decreases).

Additionally, for the same circuit parameters and $R_{vf} = 250$ kΩ, the comparison about the boundaries in the parameter space of P_0 versus C_{vf} between the pre-regulator PFC converter with a resistive load and the two-stage PFC converter are shown in Fig. 5(d). It is found that the period-doubling bifurcation in the two-stage PFC converter develops as the output power P_0 increases and its stable region is A_1, but the one in the pre-regulator PFC converter with a resistive load develops as the output power P_0 decreases and its stable region is A_1+A_2. Therefore, indeed we cannot simply extend the stability conditions of a pre-regulator PFC converter with a resistive load to a practical two-stage PFC converter.

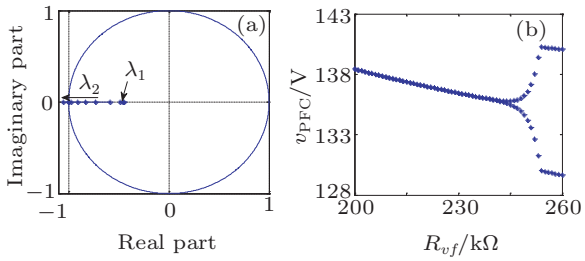


Fig. 4. The dynamical behaviours with different R_{vf}: (a) the corresponding Table 1 and (b) the bifurcation diagram.

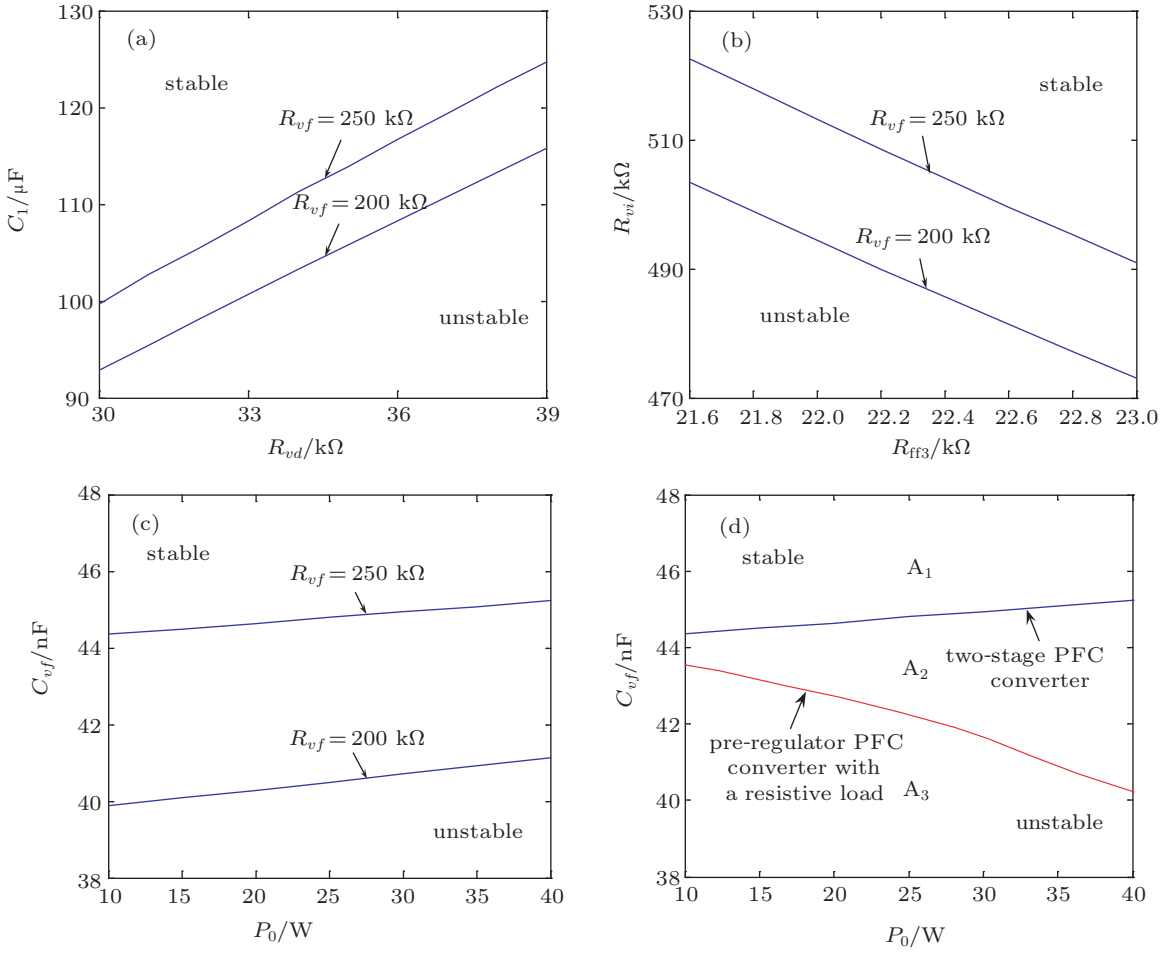


Fig. 5. The theoretical results: (a) the boundaries of the two-stage PFC converter in the parameter space of R_{vd} versus C_1; (b) the boundaries of the two-stage PFC converter in the parameter space of $R_{\rm ff3}$ versus R_{vi}; (c) the boundaris of the two-stage PFC converter in the parameter space of P_0 versus C_{vf}; (d) the comparison results between the two-stage PFC converter and the pre-regulator PFC converter with a resistive load of $R_{vf} = 250$ kΩ.

5. Experimental verification

To verify the theoretical analysis, an experimental circuit prototype of a two-stage PFC converter is constructed. The pre-regulator boost PFC converter under ACM control is accomplished by IC UC3854, and the post-regulator DC–DC Buck converter is controlled by a typical PI controller. The full schematic diagram with detailed specifications indicated is shown in Fig. 6. In our experiment, an Agilent 10074C voltage probe is used to detect the voltage $v_{\rm PFC}$, the voltage v_0, and the voltage v_{vf}. A Tektronix A622 current probe is used to detect the inductor current $i_{\rm in}$. An Agilent DSO-6014A digital oscilloscope is used to display the signals from the probes.

Firstly, according to the dictation in Section 4, the period-doubling bifurcation will occur with increasing R_{vf}. In depth, as described in Table 1, the system will operate in period-1 operation with $R_{vf} < 239.5$ kΩ. Otherwise, it will operate in period-2 operation. Let $R_{vf} = 150$ kΩ, which is smaller than the bifurcation point, the time-domain waveforms of the inductor current $i_{\rm in}$, the voltage v_{vf}, the voltage $v_{\rm PFC}$, and the voltage v_0 are shown in Fig. 7(a). It is easy to see that the system is in stable operation. Furthermore, for convenience to compare the results from the circuit experiment with the results from the IHB on the simplified model and time-integration on the complete model (Fig. 3), the value of per vertical division about the voltage v_{vf} and the voltage $v_{\rm PFC}$ are reduced, as

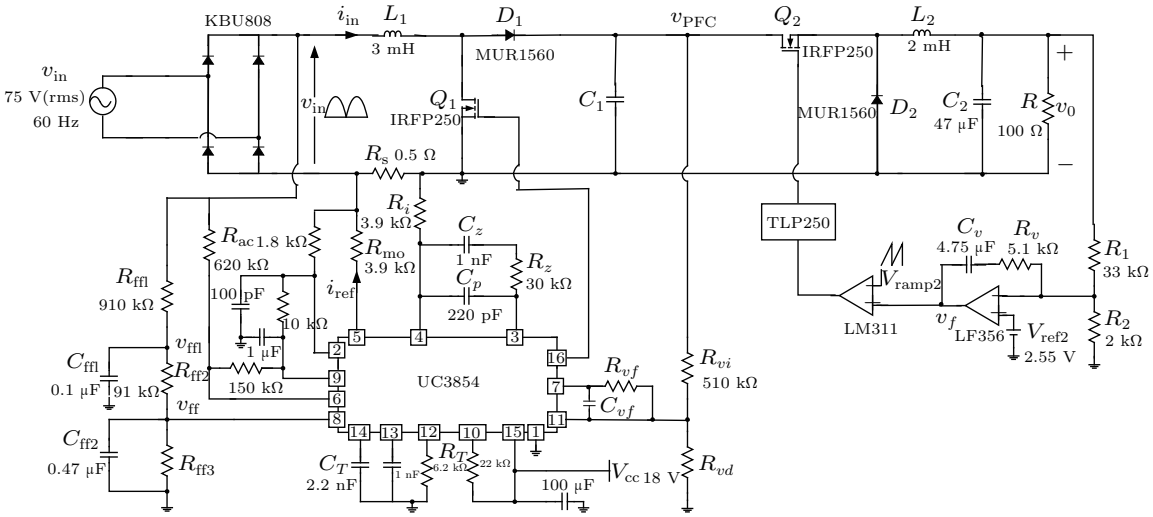


Fig. 6. Full schematic diagram of the experimental circuit.

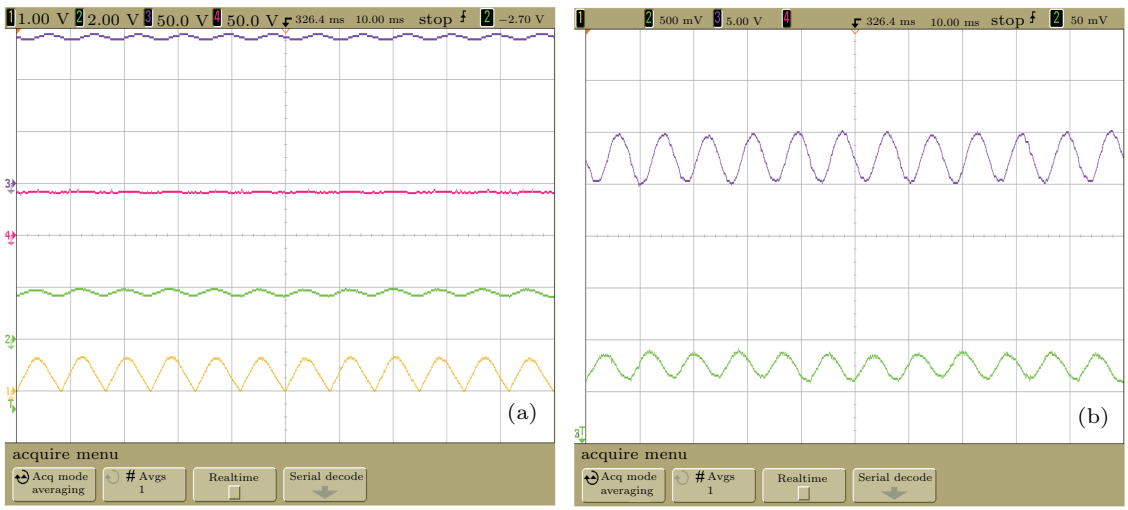


Fig. 7. Measured waveforms from the circuit experiment for $R_{vf} = 150$ kΩ; (a) the inductor current $i_{\rm in}$ (the first channel: 1 V/div), the voltage v_{vf} (the second channel: 2 V/div), the voltage $v_{\rm PFC}$ (the third channel: 50 V/div), and the voltage v_0 (the fourth channel: 50 V/div), time scale: 10 ms/div; (b) the voltage $v_{\rm PFC}$ (upper trace: 5 V/div) and the voltage v_{vf} (lower trace: 500 mV/div), time scale 10 ms/div.

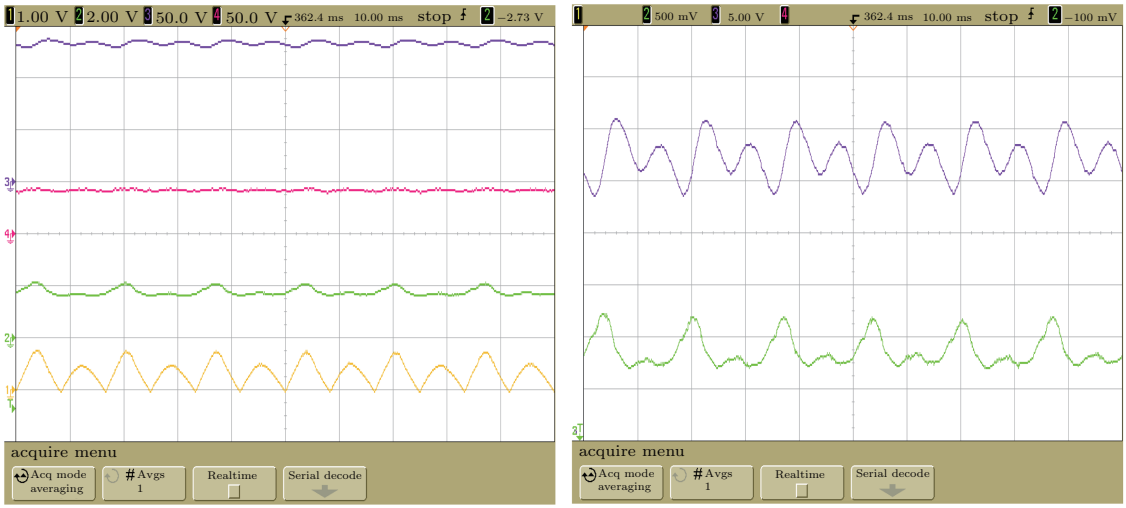


Fig. 8. Measured waveforms from the circuit experiment for $R_{vf} = 250$ kΩ: (a) the inductor current $i_{\rm in}$ (the first channel: 1 V/div), the voltage v_{vf} (the second channel: 2 V/div), the voltage $v_{\rm PFC}$ (the third channel: 50 V/div), and the voltage v_0 (the fourth channel: 50 V/div), time scale 10 ms/div; (b) the voltage $v_{\rm PFC}$ (upper trace: 5 V/div) and the voltage v_{vf} (lower trace: 500 mV/div), time scale 10 ms/div.

shown in Fig. 7(b). Obviously, the results from those three aspects are in good agreement with one other. But, when $R_{vf} = 250$ kΩ, which is bigger than the bifurcation point, the experimental results are shown in Fig. 8. It can be observed that the system is losing stability and operates in period-2 operation.

Secondly, in order to obtain the boundaries of the stable region, we locate the critical points where period-doubling bifurcation occurs. Taking $R_{vf} = 200$ kΩ, we determine the values of C_1 at the bifurcation point for different values of R_{vd}. From the results shown in Fig. 9, we see clearly that the experimental data are also in good agreement with the theoretical results. Thus, it is confirmed that the method of IHB along with Floquet theory is an effective semi-analytical one to analyse the period-doubling bifurcation in a two-stage PFC converter.

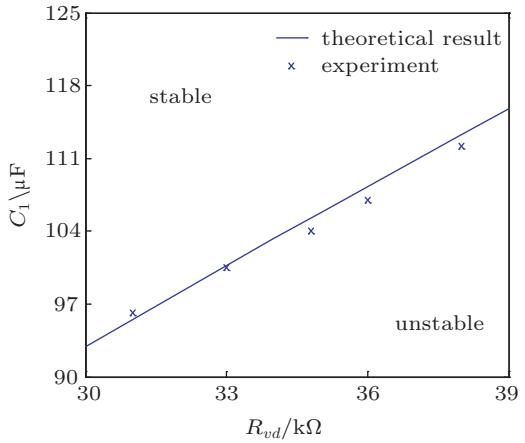


Fig. 9. Stable boundaries in the parameter space of R_{vd} versus C_1 from the theoretical result (solid line) and circuit experiment (×).

6. Conclusion

The approximate periodic solution of the simplified model, which has been derived for a two-stage PFC converter, has been calculated by using the IHB method. Then, both the period-doubling bifurcation and the bifurcation point are identified by Floquet theory. The results of time-domain voltage waveform from the time-integration, the IHB and the circuit experiment are in good agreement with one other. The results of the stable boundaries of the system from the method of IHB and Floquet theory and circuit experiment are also in good agreement with each other. In addition, by comparing with the double-averaging method, it is found that the method of IHB and Floquet theory is simpler, straightforward, easier to understand and generally applied. Therefore, the method of IHB along with Floquet theory is an effective semi-analytical method to analyse the period-doubling bifurcation in a two-stage PFC converter.

References

[1] Tse C K 2003 *Int. J. Circ. Theor. Appl.* **31** 157
[2] Ki S K, Cheng D K W and Lu D D C 2008 *IET Power Electron.* **1** 72
[3] Ren H P, Liu D 2005 *Chin. Phys.* **14** 1352
[4] Wang F Q, Zhang H, Ma X K and Li X M 2009 *Acta Phys. Sin.* **58** 6838 (In Chinese)
[5] Rustom K and Batarseh I 2003 *IEEE Int. Conf. Industr. Technol.* December 10–12, 2003, Maribor, Slovenia, Vol. 2, pp. 1089–1095
[6] Lee K Y and Lai Y S 2009 *IET Power Electron.* **2** 625
[7] Neba Y, Ishizaka K and Itoh R 2010 *IET Power Electron.* **3** 176

[8] Dranga O, Tse C K, Iu H H C and Nagy I 2003 *Int. J. Bifur. Chaos* **13** 3107
[9] EI Aroudi A, Martinez-Salamero L, Orabi M and Ninomiya T 2005 *IEEE Int. Symposium Circ. Sys.* May 23–26, 2005, Kobe, Japan, Vol. 3, pp. 2835–2838
[10] Zhang H, Ma X K, Xue B L and Liu W Z 2005 *Chaos, Solitons and Fractals* **23** 431
[11] Iu H H C, Zhou Y F and Tse C K 2003 *Int. J. Circ. Theor. Appl.* **31** 611
[12] Orabi M and Ninomiya T 2003 *IEEE Trans. Ind. Electron.* **50** 1116
[13] Mazumder S K, Nayfeh A H and Boroyevich D 2003 *IEEE Trans. Power Electron.* **18** 1063
[14] Wong S C, Tse C K, Orabi M and Ninomiya T 2006 *IEEE Trans. Cir. Sys.*-I **53** 454
[15] EI Aroudi A, Orabi M and Martinez-salamero L 2008 *Int. J. Bifur. Chaos* **18** 3073
[16] Wu X Q, Tse C K, Dranga O and Lu J N 2006 *IEEE Trans. Circ. Sys.*-I **53** 204
[17] Dai D, Li S N, Ma X K and Tse C K 2007 *IEEE Trans. Circ. Sys.*-I **54** 1724
[18] Orabi M and Ninomiya T 2004 *IEICE Trans. Commun.* E **87**-B 3506
[19] Dranga O, Chu G, Tse C K and Wong S C 2006 *Proc. 37th IEEE Power Electron. Spec. Conf.* June 18–22, 2006, Jeju, Korea, pp. 594–598
[20] Chu G, Tse C K and Wong S C 2009 *IEEE Trans. Power Electron.* **24** 469
[21] Orabi M, Haroon R and Youssef M 2008 *Proc. IEEE Appl. Power Electron. Conf. Exposition* February 24–28, 2008, Austin, Texas, USA, pp. 1389–1395
[22] Lau S L and Cheung Y K 1981 *ASME J. Appl. Mech.* **48** 959
[23] Ge Z M and Chen H H 1997 *J. Sound Vib.* **200** 121
[24] Raghothama A and Narayanan S 1999 *J. Sound Vib.* **226** 469
[25] Raghothama A and Narayanan S 2000 *Ocean Engineering* **27** 1087
[26] Xu L, Lu M W and Cao Q 2002 *Phys. Lett.* A **301** 65
[27] Shen J H, Lin K C, Chen S H and Sze K Y 2008 *Nonlinear Dyn.* **52** 403
[28] Todd P C 1999 *Unitrode Product and Applications Handbook* (Austin: Texas Instruments Incorporated) U-134 p. 3-269
[29] Itovich G R and Moiola J L 2006 *Chaos, Solitons and Fractals* **27** 647